Comparing natural and artificial carious lesions in human crowns by means of conventional hard X-ray micro-tomography and two-dimensional X-ray scattering with synchrotron radiation

Lea Maria Botta[a,b], Shane N. White[c], Hans Deyhle[a], Iwona Dziadowiec[a], Georg Schulz[a], Peter Thalmann[a], and Bert Müller[*a]
[a]Biomaterials Science Center, Department of Biomedical Engineering, University of Basel, 4123 Allschwil, Switzerland; [b]Volkszahnklinik Basel, Claragraben 95, 4005 Basel, Switzerland; [c]UCLA School of Dentistry, University of California, CA 90095-1668 Los Angeles, USA

ABSTRACT

Dental caries, one of the most prevalent infectious bacterial diseases in the world, is caused by specific types of acid-producing bacteria. Caries is a disease continuum resulting from the earliest loss of ions from apatite crystals through gross cavitation. Enamel dissolution starts when the pH-value drops below 5.5. Neutralizing the pH-value in the oral cavity opposes the process of demineralization, and so caries lesions occur in a dynamic cyclic de-mineralizing/re-mineralizing environment. Unfortunately, biomimetic regeneration of cavitated enamel is not yet possible, although re-mineralization of small carious lesions occurs under optimal conditions. Therefore, the development of methods that can regenerate carious lesions, and subsequently recover and retain teeth, is highly desirable. For the present proceedings we analyzed one naturally occurring sub-surface and one artificially produced lesion. For the characterization of artificial and natural lesions micro computed tomography is the method of choice when looking to determine three-dimensional mineral distribution and to quantify the degree of mineralization. In this pilot study we elucidate that the de-mineralized enamel in natural and artificially induced lesions shows comparable X-ray attenuation behavior, thereby implying that the study protocol employed herein seems to be appropriate. Once we know that the lesions are comparable, a series of well-reproducible *in vitro* experiments on enamel regeneration could be performed. In order to quantify further lesion morphology, the anisotropy of the enamel's nanostructure can be characterized by using spatially resolved, small-angle X-ray scattering. We wanted to demonstrate that the artificially induced defect fittingly resembles the natural carious lesion.

Keywords: Caries, de-mineralized enamel, artificial lesion, white spot, micro computed tomography, spatially resolved small-angle X-ray scattering, synchrotron radiation, removal of partial volume phenomena

INTRODUCTION

Human enamel, which is a unique, biologically and hierarchically ordered material with hydroxyapatite crystallites organized into a fibrous continuum, may remain functionally stable for decades; the crowns of human teeth have even been known to last in fossilized state for millennia. To date, human crown enamel has not been reproduced by engineering processes [1, 2]. Attacks by acidogenic bacteria generally lead to dissolution and cavitation [3, 4]. Dental caries is stated to be the most prevalent chronic childhood disease worldwide [5] and is the primary cause of oral pain and tooth loss [6-8]. The burden of dental caries lasts a lifetime, because once the tooth structure is destroyed, it will usually need restoration and additional maintenance throughout life [9]. In addition, the economic impact of such therapeutic approaches is enormous. The World Health Organization estimated that dental treatment costs accounted for 5 to 10 % of healthcare budgets in industrialized countries, notwithstanding additional costs caused through absence from work [7, 8]. So far, treatments have relied mainly on the mechanical replacement of decayed tissue by inert biomaterials, e.g. by an isotropic polymer or a ceramic composite material [10]. Small, early lesions in the enamel, termed *white spots*, often go untreated in the hope that the attack can be stopped by natural re-mineralization and a less cariogenic diet [11]. Figure 1 explains schematically the morphology of a human molar with an enamel lesion and the notations for the directions used by dentists.

*bert.mueller@unibas.ch; phone +41 61 207 5430; fax 41 61 207 5499; www.bmc.unibas.ch

Developments in X-Ray Tomography X, edited by Stuart R. Stock, Bert Müller, Ge Wang, Proc. of SPIE Vol. 9967, 99670S · © 2016 SPIE · CCC code: 0277-786X/16/$18 · doi: 10.1117/12.2238487

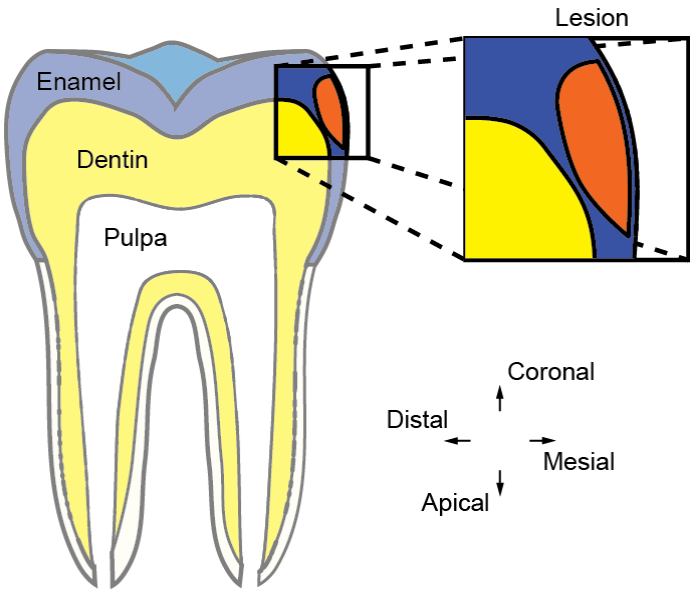

Figure 1. The scheme of a human crown (molar) shows the hard enamel (blue color) and the softer dentin (yellow color). The early lesion, shown in red color, usually exhibits an intact shell, clearly visible in the magnified part. The four directions, using the nomenclature of dentists, are indicated. The lesion is either a bacteria-induced demineralized part of enamel or an artificially induced defect, as presented schematically. Once the lesion passes the dental-enamel junction, it spreads out faster into the dentin than in the enamel.

Such an enamel lesion has characteristic features. Because of cyclic de- and re-mineralization and the superimposed overall demineralization process, the outer surface of an early lesion usually remains as a hard shell (see inset of Figure 1). Thus, natural lesions occur in a dynamic cyclic de-mineralizing/re-mineralizing environment and grow until, finally, they have to be treated [12]. Nowadays, the dentist treats a carious lesion by mechanically removing the affected hard tissues and replacing the relevant part of the crown using more or less established inert biomaterials [10]. This is generally associated with the additional removal of healthy hard-tooth tissue adjoining the lesion. Furthermore, as the current restoration materials do not match the performance of natural and healthy hard tissues, their limited lifespans make further interventions necessary [13, 14]. Therefore, the development of methods to regenerate carious lesions, and repair and retain teeth, is highly sought after. Non-invasive intervention methods are coming more and more to the fore, although applications in this domain are still rather limited [11].

Natural analog, or biomimetic, re-mineralization is important, because enamel is a highly complex fibrous composite-ceramic, highly ordered and oriented on both the micro- and nanometer scales, and designed for optimal toughness and wear resistance [15]. Simply replacing lost crystallites with amorphous hydroxyapatite will reproduce neither the remarkable natural structure nor its functional capability. Recently, it has been shown that demineralized enamel, even in moderately sized carious lesions, retains all of its complex nano-structural spatial organization, so natural analog or biomimetic re-mineralization is now—albeit in principle—possible [1]. Nonetheless, this task is not a trivial undertaking and will require significant research efforts.

Recently, peptides, which form supra-molecular, three-dimensional networks, were reported to provide an organic matrix improving the re-mineralization of early carious lesions in dental enamel [16]. One of these self-assembling peptides, P 11-4, is shown to form supra-molecular, three-dimensional networks in response to acidic conditions present within the cavities of carious lesions [17, 18]. The biomimetic, scaffold-like structures of P 11-4 should trigger hydroxyapatite nucleation along its fiber axes, thus resulting in a regenerative padding of the lesion with nanometer-sized crystalline minerals [18]. Recent data have demonstrated that this technique facilitates crystallite formation from the ionic species present in saliva, hence supporting the repair of the lesion in a nature-analog manner [16].

In order to develop or optimize any re-mineralization procedure, a protocol for reliable *in vitro* studies is required. Researchers want to study not only naturally occurring lesions, such as early white spot lesions occasionally found in

extracted human teeth, but also intentionally induced standardized artificial lesions made on extracted teeth *in vitro.* As naturally occurring lesions exhibit variety in their structure [19], we chose to include a lesion artificially induced according to an established protocol [20]. This approach will provide comparability for future studies and the existing literature. In addition, a smooth natural enamel caries lesion (white spot) was investigated to ensure the validity of the model. We hypothesize that the defects, which were generated after tooth extraction *in vitro*, which means within a period of several days, show behavior that differs from the natural lesions found on the same human tooth, formed over months and years influenced by thousands of de- and re-mineralization cycles.

In order to develop a sound basis on which to prove our hypothesis, selected parts of the crown were characterized by means of conventional high-resolution micro computed tomography and spatially resolved small-angle X-ray scattering (SAXS), using synchrotron radiation.

Micro computed tomography (μCT) is the method of choice when looking to measure three-dimensional local X-ray attenuation, which directly relates to mineral distribution in human crown tissue. Furthermore, it enables us to quantify the degree of mineralization within the healthy enamel and dentin as well as in a natural or artificial lesion. If changes in mineralization should be studied, the datasets obtained before and after such changes have to be registered in three-dimensional space [21], in order to extract the common volume and to locate the areas of re- and de-mineralization [22] for direct comparison. Consequently, μCT can support the evaluation of mineralization protocols.

For optimized therapeutic outcomes, re-mineralization should be biomimetic. This necessitates characterization of the abundance and orientation of nanometer-sized minerals in the treated lesions. Spatially resolved SAXS allows for non-destructively investigating the average orientation and degree of nanostructure anisotropy present in human tooth enamel [1, 2, 10, 13, 19, 23] and is therefore an indispensable tool to characterize the efficiency of currently available and future biomimetic treatment strategies.

MATERIALS AND METHODS

Human tooth selection

A naturally occurring carious lesion and an artificially induced surface lesion, obtained from the same molar, were used. All procedures were conducted in accordance with the Declaration of Helsinki and according to the ethical guidelines of the Canton of Basel, Switzerland. The approval of the study protocol was numbered 290/13 by the responsible Ethical Committee. The tooth had been scheduled for extraction due to clinical reasons unrelated to the study. Written consent by patient for the use of the extracted tooth was given in the patient registration form of the Volkszahnklinik, Basel, Switzerland.

De-mineralization protocol and slicing

Immediately after extraction, the molar was immersed in a 0.1% thymol solution. Soft tissue, calculus, and alveolar bone remaining on the extracted tooth were removed using a scalpel.

As displayed in Figure 2, artificial lesions in human teeth were generated by painting the respective tooth with a layer of nail varnish, leaving an approximately 2 mm × 2 mm window. Subsequently, the teeth were incubated for a period of three days in acidic demineralization buffer (50 mM acetic acid, 2.2 mM $CaCl_2$, 2.2 mM NaH_2PO_4 titrated with 1 M KOH to pH 4.4). Tooth slices were obtained by cutting with a band saw (Exakt Apparatebau GmbH, Norderstedt, Germany). These slices were approximately 500 μm thick and stored in water before and during measurements to prevent drying. All chemicals used in the present study were supplied by Sigma-Aldrich Co. LLC.

Micro computed tomography

The tooth slices were individually transferred into a water-filled Eppendorf tube to maintain a wet environment and prevent drying. This Eppendorf tube was closed and glued onto a holder placed into the manipulator of the μCT-system.

Micro computed tomography datasets were acquired using a nanotom® m (phoenix|x-ray, GE Sensing & Inspection Technologies GmbH, Wunstorf, Germany). The pixel size corresponded to 7.0 μm, selected according to the maximal diameter of the tooth slice. Therefore, the field of view corresponded to 21.0 mm × 16.8 mm. A 0.2 mm-thick copper filter was placed in the beam path to increase mean photon energy and reduce beam hardening. For all specimens, the acceleration voltage was set to 90 kV and the electron beam current to 260 μA [24, 25]. The number of radiographs

(projections), acquired with constant angular steps along 360°, was set to 1,200. The acquired data were reconstructed with Phoenix datos|x 2.0 reconstruction software as provided by the supplier of the nanotom® m.

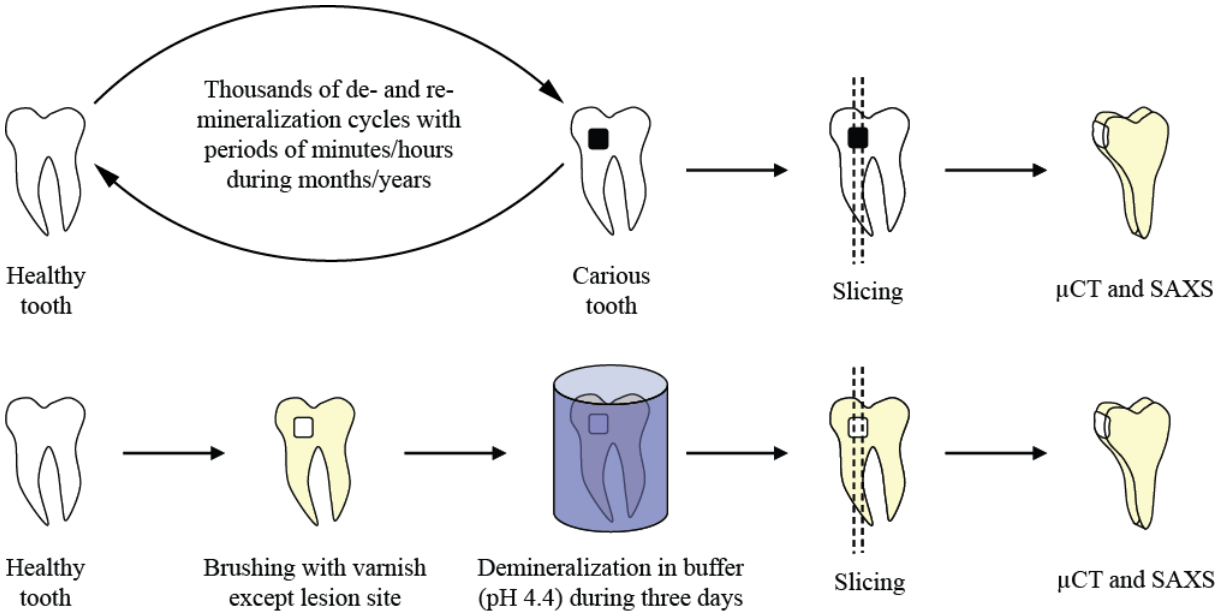

Figure 2. The formation of a caries lesion is generally a process which incorporates thousands of de-mineralization cycles dominated by de- versus re-mineralization. Tooth extraction in the early stages of caries is rather infrequent and often includes mechanical damage as the result of the dentist's intervention. Therefore, using healthy enamel and applying a de-mineralization procedure in a well-defined manner, as specified in the second row, allows reliable studies on quality-reduced enamel. In this study, the slices with the artificially induced and the natural lesions were examined comparably by means of conventional hard X-ray micro computed tomography and cutting-edge spatially resolved X-ray scattering at the Swiss Light Source, Villigen, Switzerland.

Coherent small-angle X-ray scattering

Small-angle X-ray scattering measurements were performed at the cSAXS beamline of the Swiss Light Source (Paul Scherrer Institute, Villigen, Switzerland) [26]. The specimens were stored in polyimide sachets, as one can see by the characteristic color on the photograph in Figure 3, placed on an aluminum frame, and then raster-scanned in 30 µm × 10 µm steps in horizontal and vertical directions (x and y) through an 18.6 keV X-ray beam focused to 30 µm × 10 µm full-width-at-half-maximum spot size at the specimen location. The specimen-detector distance D_{sd} of 7.1 m was determined following the first scattering order of a silver behenate specimen at the specimen position (see Figure 3). To reduce air scattering, an evacuated flight tube was placed between the specimen and the detector.

This measurement method, as described schematically in Figure 3, allowed for assessing many essential nanostructure parameters, including their size, orientation, and abundance [2]. In the scope of this study, however, the ability to characterize anisotropy was the primary aim.

RESULTS

Micro computed tomography of crown slices

Conventional micro computed tomography served for the measurement of the local degree of mineralization within the approximately 500 µm-thick crown slices. Selected slices of the tomography data from the artificial and the natural lesions are presented in Figures 4 and 5, respectively. These images show the characteristic microstructure of lesions, i.e. the areas of reduced mineral content. Below a more highly mineralized shell with a thickness of a few ten micrometers one can recognize the demineralized zone, which is about 50 µm thick for the artificial lesion and has an extension of about 250 µm for the natural lesion.

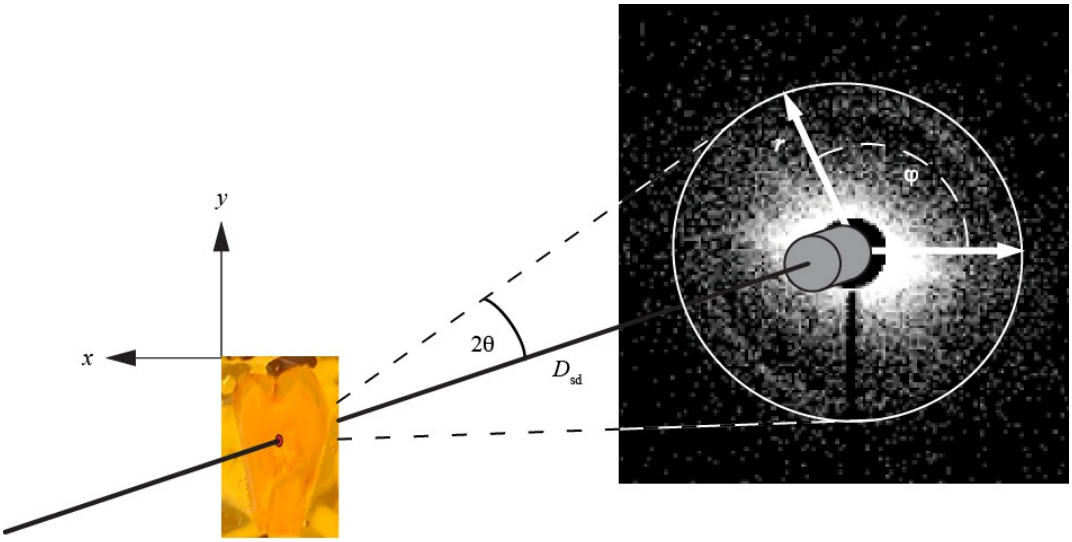

Figure 3. Scheme of the experimental setup for spatially resolved SAXS. A monochromatic X-ray beam penetrates the tooth slice, including the sachet and water, and is stopped in front of the detector by the beam stop. A small part of the X-ray beam is scattered by the nanometer-size components of the tooth slice along its path through the crown tissues. It has been shown that the sachet and water have no impact. For the smaller nanostructures one finds larger scattering angles θ related to the radius *r*. If there is a preferential orientation of the nanostructure of interest the related ring shows varying intensity. Spatial resolution in real space is obtained by moving the tooth slice in *x* and *y* directions.

The tooth slice with the natural lesion exhibits many defects which most probably arise from the usage of the forceps for the extraction. It is difficult to avoid the occurrence of such cracks, especially if the enamel is demineralized. One can even find such cracks in extracted intact teeth [27].

In order to quantify the degree of mineralization within the three-dimensional region of interest, we generated a histogram of the local X-ray attenuation values in the voxels of a volume of interest. These data are displayed on the left in Figures 4 and 5, respectively. It should be noted that the grayscale bars above the histograms correspond exactly to the gray values used in the two images on the right of Figures 4 and 5. Therefore, the imaging data can be directly related to the peaks and shoulders in the histograms.

The histograms can be reasonably fitted using three Gaussians. This fit is given in black. The three Gaussians are red-, blue-, and gray-colored. The gray peak on the left corresponds to the water surrounding the slices of the crown. The enamel-related peak, which is blue-colored, has a shoulder, *cp.* red-colored peak, towards lower X-ray absorption values. Therefore, one can conclude that this red-colored peak relates to the lesion and to the partial volumes at interfaces. The position of this peak related to water and sound enamel is well comparable for the artificial and natural lesions. Analyzing the area below the peak of the red-colored Gaussian, an estimate of the volume of the lesion can be given. As first approach, intensity-based thresholding [28] was applied. The intersection points between the fitted Gaussians were selected as lower and upper threshold, cf. vertical yellow-colored lines in the histograms of Figs. 4 and 5, and all voxels presenting gray values within this range were considered to be part of the lesion. The resulting volumes amount to 1.7×10^5 voxels or $0.057\ \mathrm{mm}^3$ for the artificial and 1.9×10^5 voxels or $0.065\ \mathrm{mm}^3$ for the natural lesions. The corresponding voxels are overlaid to the original gray-scaled imaging data using the red and yellow colors in Figures 4 and 5, right hand side. It is apparent that this approach overestimates the lesion's volume, as also the specimens' surfaces are included due to partial volume effects. Therefore, the values given above can only be regarded as an upper limit. A conservative approach was obtained by applying image opening, i. e. erosion followed by dilation, to the segmentation masks, resulting in the red-colored overlay only. Resulting volumes were 4.5×10^4 voxels ($0.016\ \mathrm{mm}^3$) for the artificial lesion and 5.3×10^4 voxels ($0.018\ \mathrm{mm}^3$) for the natural one. This approach rather underestimates the lesions' volume. Thus, these volumes can bee interpreted as the lower limits. The mean gray value of the red-colored areas is in reasonable agreement with the positions of the intermediate, red-colored Gaussians. Therefore, we reasonably conclude that the degree of de-mineralization is comparable for the naturally formed and the artificially induced lesions.

The full-width-at-half maxima of water in the sachet, which surrounds the tooth slice, and of unaffected enamel, are similar. The peaks of the affected enamel are broader than the peaks of the enamel and water, thereby indicating a varying degree of de-mineralization throughout the lesions.

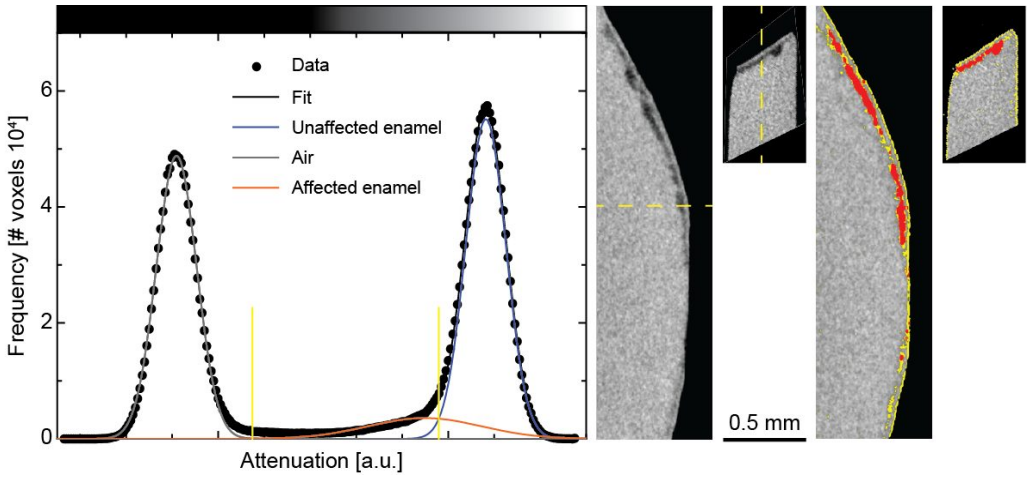

Figure 4. The images on the right of the diagram show two selected µCT-slices from the crown with the artificially induced lesion in two perpendicular directions, as indicated by the yellow-colored dashed lines. The histogram containing the three-dimensional datasets exhibits one water-related peak without a shoulder and one enamel-related peak with a shoulder at lower X-ray absorption values, which arises as a result of de-mineralization and partial volume effects. The segmentation of this peak-based thresholding overestimates the lesion's volume (yellow mask in the images on the right plus the red-colored areas). A conservative estimate is obtained after image opening (red-colored region).

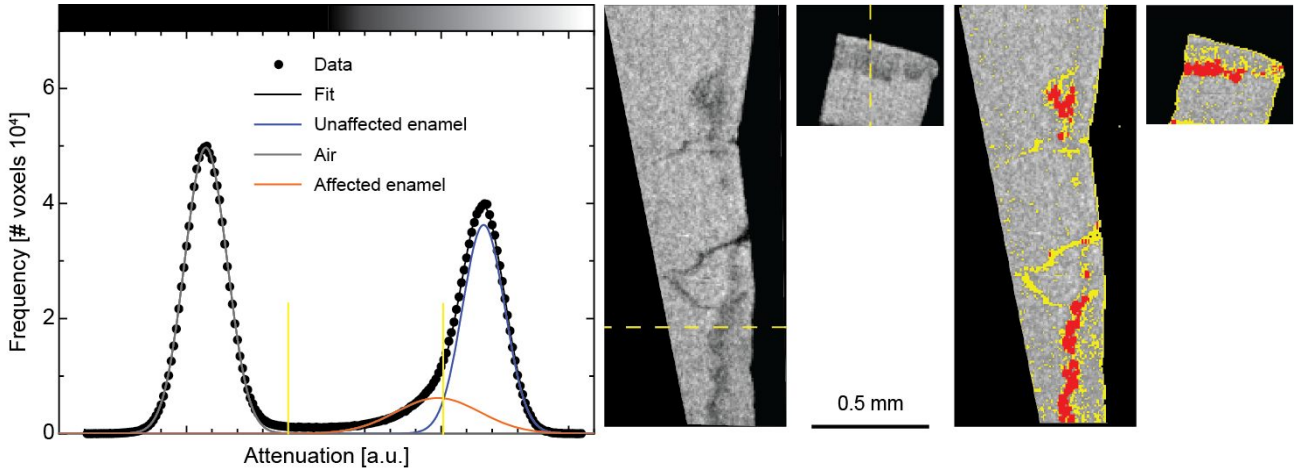

Figure 5. The images on the right of the diagram show two selected µCT-slices from the crown piece with the natural lesion in two perpendicular directions, as indicated by the yellow-colored dashed lines. The images display not only the demineralized regions of the carious lesion but also further defects such as extended cracks, which probably formed during tooth extraction. The histogram containing the three-dimensional datasets exhibits one water-related peak without a shoulder and one enamel-related peak with a shoulder at lower X-ray absorption values, which arises from caries-induced de-mineralization. The segmentation of this peak-based thresholding overestimates the lesion's volume (yellow mask in the images on the right plus the red-colored areas). A conservative estimate is obtained after image opening (red-colored region).

Spatially resolved small-angle X-ray scattering of crown slices

The 500 µm-thick tooth slices used for the µCT study were also investigated using synchrotron radiation-based small-angle X-ray scattering in transmission mode, to evaluate the anisotropy and the orientation of the nanostructures of the crown slices. Small-angle X-ray scattering has proven to be a valuable imaging technique for hard tissue on the nanometer scale, such as for bone or teeth [29]. Selected data from our study are displayed in Figure 6.

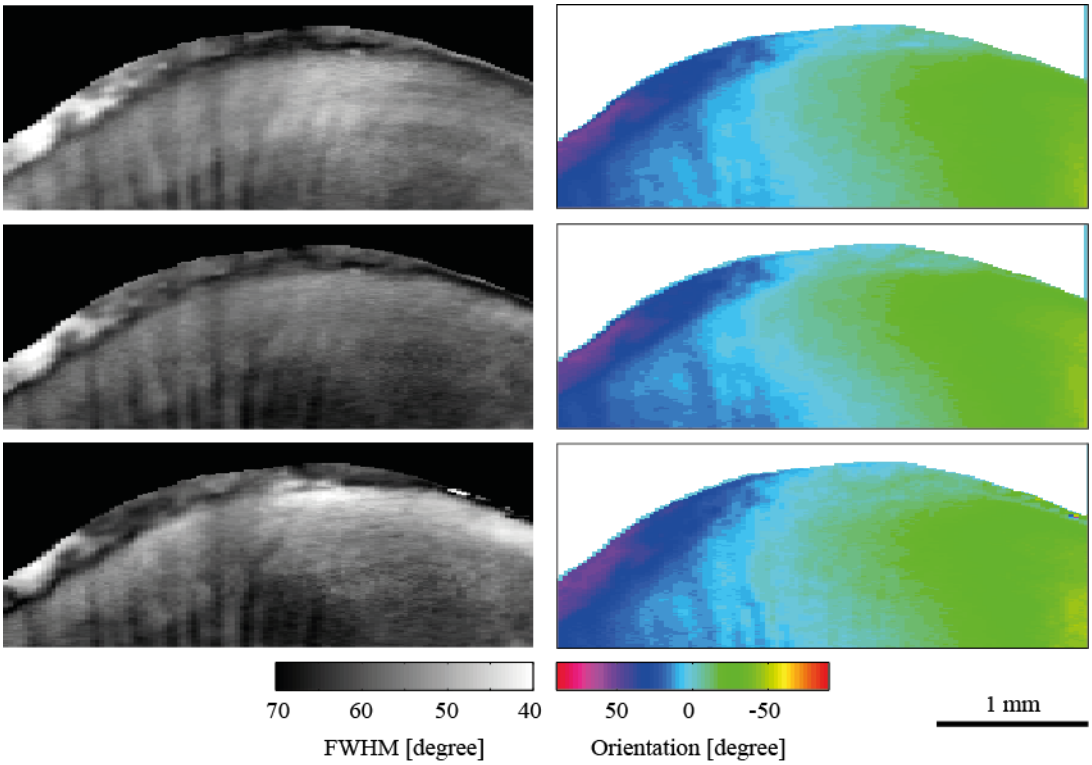

Figure 6. The images of the spatially resolved SAXS data from the artificial lesion show characteristic anatomical features. The left column represents anisotropy for periodicities ranging from 40 to 50 nm, from 90 to 100 nm, and from 100 to 150 nm, respectively. The right column displays the corresponding orientation data using the color code given below. Note the area investigated corresponds to a significant part of the human crown, *cp.* length bar.

Figure 6 is composed of six images from a tooth slice with the artificial lesion. The first row shows data that correspond to periodicities ranging from 40 to 50 nm. The second row displays the related images, simultaneously measured, covering a range of periodicities between 90 and 100 nm, whereas the data related to a periodicity of 100 to 150 nm are represented in the third row.

The gray-scale images in the first column exhibit the spatial distribution of the full-width-at-half-maximum (FWHM) of the azimuthal SAXS intensity [19] according to the angle-gray value scale below. This information is related to the degree of orientation and can be regarded as an appropriate measure of the preferential orientation or the anisotropy of the crown's nanostructures in the projection plane. In essence, the smaller the FWHM, the better ordered the nanostructures. It is notable that regions containing carious enamel exhibit higher anisotropy than the healthy part of the crown.

The images in the right column refer to the orientation of the nanostructures according to the color bar given below. Zero degree means the domination of the vertically oriented nanostructures. Likewise, one can compose images from a human crown slice with a natural lesion.

The images in the right column of Figure 6 show a change in the orientation between 90°, pointing to the left, and -90°, pointing to the right, namely orientation from left to right within each slice. This means that the nanostructures have an orientation perpendicular to the tooth surface, which is consistent with the dominant angle of the crystallites within enamel rods.

The images contain the characteristic anatomy of human teeth, which allows for easier alignment by dental experts. Because some features can also be found in the tomography data, registration between the spatially resolved SAXS data and the projection of the tomography data is feasible [24]. The lower X-ray absorption within the lesion relates to higher scattering in the spatially resolved SAXS data, which implies the X-ray scattering at pores of nanometer size. Consequently, the two methods are considered to be complementary.

DISCUSSION AND CONCLUSION

The present study on one human tooth crown demonstrates that artificial caries lesions, which closely resemble the natural state, can be prepared with reasonable ease. The size of the white spot lesion can be controlled with reasonable precision, too, given that the artificial lesion, generated within a period of 72 hours, was comparable in volume to the selected natural lesion. Dowker *et al.* [30] demonstrated in an *in vitro* study almost two decades ago that the size of lesions could be simply controlled through the exposure time to the selected acidic species. It is thus possible to generate lesions, which closely resemble the natural state concerning size. It has, however, to be taken care that the degree of mineral loss matches that of natural lesions, as the mineral loss of an artificially produced lesion is inhomogeneous with respect to the position on the human tooth surface exposed to acid. The process of de-mineralization is expected to be complex, even in simplified *in vitro* models as shown more than a decade ago [31]. In agreement with the results of the present investigation, Dowker *et al.* [31] found a 50 µm-thin intact surface layer with a significantly higher mineral density than the underlying enamel.

The natural and artificial lesions of the present investigation and of many previously performed *in vitro* experiments show comparable behavior. The surface layers are essentially intact, and the X-ray attenuation is well comparable and associated with increased X-ray scattering intensity within the lesions. Crabb *et al.* [32] noted the similar histological appearance, under polarized light, of artificially induced enamel lesions to those found in carious lesions. So far, a variety of artificial carious lesions has been studied. As already pointed out in 1983 by Featherstone *et al.*, these artificial lesions appeared to match the classic natural regional description of natural lesions [33].

Diffraction and scattering techniques based on X rays have been widely used to study the anisotropy of nanometer-size crystallites in slices of intact human crowns [34, 35] and slices of human crowns with carious lesions [35, 36]. In agreement with the present study, it was observed that the X-ray scattering potential of enamel lesions is significantly higher than that of unaffected enamel, associated with increased nanometer-scale porosity within the lesion [1, 19, 37].

The combination of the two experimental techniques in the present study, i.e. micro computed tomography and synchrotron radiation-based spatially resolved X-ray scattering, not only permits the evaluation of the degree of mineralization, but also provides conclusions on the orientation of the nanostructures within the hard tissues of the human teeth. No significant alteration between the main orientation of the scattering signal in carious and unaffected enamel was found for the artificial lesion, whereas some differences in anisotropy exist. This statement is in agreement with experimental data from diffraction [37].

Although spatially resolved small- and wide-angle X-ray scattering has proven to be a valuable imaging technique for determining the nanometer-size features of biomaterials and tissues, such as bone, teeth, and brain matter [29], it remains constrained to two dimensions. Very recently, though, an approach has been proposed to extend SAXS to the third dimension [38]. Liebi *et al.* [39] introduced an imaging method that combines SAXS with tensor tomography and allows for three-dimensional reciprocal space imaging [39]. Schaff *et al.* have followed in the same issue of Nature with a similar approach, taking advantage of the rotation invariance of the scattering signal parallel to the rotation axis [38]. These methods promise a better understanding of mesoscopic structures in human tissues such as bone or teeth, and although they are time-consuming and difficult to understand/implement, we are convinced that these sophisticated techniques will help improve our understanding of the formation and repair of caries lesions. This future knowledge on three-dimensionally ordered nanostructures will promote the development of biologically inspired dental fillings [10] and biomimetic tooth repair.

To ensure the efficient use of the available beam time at synchrotron radiation facilities, protocols should be first verified using powerful, conventional micro computed tomography setups. Additionally, the adaptation of the protocol from entire crowns with quality reduced enamel and dentin parts to slices significantly less than a millimeter thick is challenging and needs further improvement. Given the interest in non-invasive treatments of white spot enamel lesions, a clinical procedure using appropriate materials needs to be developed for non-destructive modification of the surface layer of these white spot enamel lesions to increase porosity of the top layers and to improve the mineralization below the shell. The development of less invasive alternatives for the treatment of dental caries is still an important challenge. The challenge does even exist for the white spot lesions, since the carious defects are highly variable even with extensions into the dentin and comprise surface layers of considerable thickness [40]. One study on potential treatments of enamel lesions was performed by Veira *et al.* [41]. They showed that repeated irradiation with a carbon dioxide laser might enhance the inhibition of enamel de-mineralization. The physical changes and the organic blocking effect can reduce the enamel de-mineralization until the temperature threshold of 400 °C was achieved [41].

ACKNOWLEDGMENTS

The technical support of F. Schmidli (Basel) for the tooth preparation is gratefully acknowledged. Extracted teeth were kindly provided by M. Jakobs (The Volkszahnklinik, Basel, Switzerland). Experiments were performed on the cSAXS beamline at the Swiss Light Source (proposal numbers 20131216 and 20131056), Paul Scherrer Institut, Villigen, Switzerland, with generous scientific and technical support provided by O. Bunk, M. Liebi and M. Guizar-Sicairos. The authors would also like to thank L. Kind and U. Pieles for their support in the preparative and experimental phases of the project. The Swiss Nanoscience Institute and the Swiss National Science Foundation (SNSF) partially financed the research activities within the *nanocure* project (Project No. 144617).

REFERENCES

[1] Deyhle, H., Bunk, O., and Müller, B., "Nanostructure of healthy and caries-affected human teeth," Nanomedicine: Nanotechnology, Biology, and Medicine **7**, 694-701 (2011).

[2] Gaiser, S., Deyhle, H., Bunk, O., White, S. N., and Müller, B., "Understanding nano-anatomy of healthy and carious human teeth: A prerequisite for nanodentistry," Biointerphases **7**, 4 (2012).

[3] Featherstone, J. D., "Dental caries: A dynamic disease process," Australian Dentistry Journal **53**, 286-291 (2008).

[4] Forssten, S. D., Bjorklund, M., and Ouwehand, A. C., "Streptococcus mutans, caries and simulation models," Nutrients **2**, 290-298 (2010).

[5] Bagramian, R. A., Garcia Godoy, F., and Volpe, A. R., "The global increase in dental caries. A pending public health crisis," American Journal of Dentistry **22**, 3-8 (2009).

[6] Petersen, P. E., "The burden of oral disease: Challenges to improving oral health in the 21st century," Bulletin of the World Health Organization **83**, 3 (2005).

[7] Petersen, P. E., "World Health Organization global policy for improvement of oral health--World Health Assembly 2007," International Dentistry Journal **58**, 115-121 (2008).

[8] Petersen, P. E., "Global policy for improvement of oral health in the 21st century--implications to oral health research of World Health Assembly 2007, World Health Organization," Community of Dental Oral Epidemiology 37, 1-8 (2009).

[9] Selwitz, R. H., Ismail, A. I., and Pitts, N. B., "Dental caries," Lancet **369**, 51-59 (2007).

[10] Deyhle, H., Bunk, O., Buser, S., Krastl, G., Zitzmann, N., Ilgenstein, B., Beckmann, F., Pfeiffer, F., Weiger, R., and Müller, B., "Bio-inspired dental fillings," Proceedings of SPIE **7401**, 74010E (2009).

[11] Cochrane, N. J., Cai, F., Huq, N. L., Burrow, M. F., and Reynolds, E. C., "New approaches to enhanced remineralization of tooth enamel," Journal of Dental Research **89**, 1187-1197 (2010).

[12] Makinen, K. K., "Sugar alcohols, caries incidence, and remineralization of caries lesions: A literature review," International Journal of Dentistry **2010**, 981072 (2010).

[13] Deyhle, H., Hieber, S., and Müller, B., [Nanodentistry] Springer Science+Business Media B.V., Berlin Heidelberg (2012).

[14] Sunnegardh-Gronberg, K., van Dijken, J. W. V., Funegard, U., Lindberg, A., and Nilsson, M., "Selection of dental materials and longevity of replaced restorations in Public Dental Health clinics in Northern Sweden," Journal of Dentistry **37**, 673-678 (2009).

[15] White, S. N., Luo, W., Paine, M. L., Fong, H., Sarikaya, M., and Snead, M. L., "Biological organization of hydroxyapatite crystallites into a fibrous continuum toughens and controls anisotropy in human enamel," Journal of Dental Research **80**, 321-326 (2001).

[16] Brunton, P. A., Davies, R. P., Burke, J. L., Smith, A., Aggeli, A., Brookes, S. J., and Kirkham, J., "Treatment of early caries lesions using biomimetic self-assembling peptides--a clinical safety trial," British Dental Journal **215**, E6 (2013)..

[17] Firth, A., Aggeli, A., Burke, J. L., Yang, X., and Kirkham, J., "Biomimetic self-assembling peptides as injectable scaffolds for hard tissue engineering," Nanomedicine (London) **1**, 189-199 (2006).

[18] Kirkham, J., Firth, A., Vernals, D., Boden, N., Robinson, C., Shore, R. C., Brookes, S. J., and Aggeli, A., "Self-assembling peptide scaffolds promote enamel remineralization," Journal of Dental Research **86**, 426-430 (2007).

[19] Deyhle, H., White, S. N., Bunk, O., Beckmann, F., and Müller, B., "Nanostructure of the carious tooth enamel lesion," Acta Biomaterialia **10**, 355-365 (2014).

[20] Chow, L. C., "Diffusion of ions between two solutions saturated with respect to hydroxyapatite: A possible mechanism for subsurface demineralization of teeth," Journal of Research of NIST **115**, 217-224 (2010).

[21] Müller, B., Deyhle, H., Lang, S., Schulz, G., Bormann, T., Fierz, F., and Hieber, S., "Three-dimensional registration of tomography data for quantification in biomaterials science," International Journal of Materials Research **103**, 242-249 (2012).

[22] Stalder, A., Ilgenstein, B., Chicerova, N., Deyhle, H., Beckmann, F., Müller, B., and Hieber, S. E., "Combined use of micro computed tomography and histology to evaluate the regenerative capacity of bone grafting materials," International Journal of Materials Research **105**, 679-691 (2014).

[23] Müller, B., Deyhle, H., Bradley, D., Farquharson, M., Schulz, G., Muller-Gerbl, M., and Bunk, O., "Scanning x-ray scattering: Evaluating the nanostructure of human tissues," European Journal of Nanomedicine **3**, 30-33 (2010).

[24] Deyhle, H., Dziadowiec, I., Kind, L., Thalmann, P., Schulz, G., and Müller, B., "Mineralization of early stage carious lesions in vitro - A quantitative approach," Dentistry Journal **3**, 111-122 (2015).

[25] Dziadowiec, I., Beckmann, F., Schulz, G., Deyhle, H., and Müller, B., "Characterization of a human tooth with carious lesions using conventional and synchrotron radiation-based micro computed tomography," Proceedings of SPIE **9212**, 92120W (2014).

[26] Bunk, O., Bech, M., Jensen, T. H., Feidenhans'l, R., Binderup, T., Menzel, A., and Pfeiffer, F., "Multimodal x-ray scatter imaging," New Journal of Physics **11**, 123016 (2009).

[27] Kühl, S., Deyhle, H., Zimmerli, M., Spagnoli, G., Beckmann, F., Müller, B., and Filippi, A., "Cracks in dentin and enamel after cryo-preservation," Oral Surgery, Oral Medicine, Oral Pathology, Oral Radiology and Endodontology **113**, e5-e10 (2011).

[28] Müller, B., Beckmann, F., Huser, M., Maspero, F., Szekely, G., Ruffieux, K., Thurner, P., and Wintermantel, E., "Non-destructive three-dimensional evaluation of a polymer sponge by micro-tomography using synchrotron radiation," Biomolecular Engineering **19**, 73-78 (2002).

[29] Fratzl, P., Jakob, J. F., Rinnerthaler, S., Roschger, P., and Klaushofer, K., "Position-resolved small-angle X-ray scattering of complex biological materials," Journal of Applied Crystallography **30**, 765-769 (1997).

[30] Dowker, S. E. P., Anderson, P., and Elliott, J. C., "Real-time measurement of in vitro enamel demineralization in the vicinity of the restoration-tooth interface," Journal of Materials Science: Materials in Medicine **10**, 379-382 (1999).

[31] Dowker, S. E. P., Elliott, J. C., Davis, G. R., and Wassif, H. S., "Longitudinal study of the three-dimensional development of subsurface enamel lesions during in vitro demineralisation," Caries Research **37**, 237-245 (2003).

[32] Crabb, H. S., and Darling, A. I., "X-ray absorption studies of human dental enamel," Oral Surgery, Oral Medicine, Oral Pathology **9**, 995-1009 (1956).

[33] Featherstone, J. D., ten Cate, J. M., Shariati, M., and Arends, J., "Comparison of artificial caries-like lesions by quantitative microradiography and microhardness profiles," Caries Research **17**, 385-391 (1983).

[34] Al-Jawad, M., Streuwer, A., Kilconey, S. H., Shore, R. C., Cywinski, R., and Wood, D. J., "2D mapping of texture and lattice parameters of dental enamel," Biomaterials **28**, 2908-2914 (2007).

[35] Märten, A., Fratzl, P., Paris, O., and Zaslansky, P., "On the mineral in collagen of human crown dentine," Biomaterials **31**, 5479-5490 (2010).

[36] Yagi, N., Ohta, T., Matsuo, T., Tanaka, T., Terada, Y., Kamasaka, H., To-o, K., Kometani, T., and Kuriki, T., "Evaluation of enamel crystallites in subsurface lesion by microbeam X-ray diffraction," Journal of Synchrotron Radiation **16**, 398-404 (2009).

[37] Tanaka, T., Yagi, N., Ohta, T., Matsuo, Y., Terada, H., Kamasaka, K., To-o, K., Kometani, T., and Kuriki, T., "Evaluation of the distribution and orientation of remineralized enamel crystallites in subsurface lesions by X-ray diffraction," Caries Research **44**, 253-259 (2010).

[38] Schaff, F., Bech, M., Zaslansky, P., Jud, C., Liebi, M., Guizar-Sicairos, M., and Pfeiffer, F., "Six-dimensional real and reciprocal space small-angle X-ray scattering tomography," Nature **527**, 353-356 (2015).

[39] Liebi, M., Georgiadis, M., Menzel, A., Schneider, P., Kohlbrecher, J., Bunk, O., and Guizar-Sicairos, M., "Nanostructure surveys of macroscopic specimens by small-angle scattering tensor tomography," Nature **527**, 349-352 (2015).

[40] Cochrane, N. J., Anderson, P., Davis, G. R., Adams, G. G., Stacey, M. A., and Reynolds, E. C., "An X-ray microtomographic study of natural white-spot enamel lesions," Journal of Dental Research **91**, 185-191 (2012).

[41] Vieira, K. A., Steiner-Oliveira, C., Soares, L. E. S., Rodrigues, L. K. A., and Nobre-dos-Santos, M., "In vitro evaluation of enamel demineralization after several overlapping CO_2 laser applications," Lasers in Medical Science **30**, 901-907 (2015).